Electronic Supplementary Material (ESI) for Chemical Communications.

Supporting Information

Tailoring the growth route of lithium peroxide through the rational design of the sodium-doped nickel phosphate catalyst for lithium-oxygen batteries

Se-Si Li, Xing-He Zhao, Kai-Xue Wang,* and Jie-Sheng Chen*

Shanghai Electrochemical Energy Devices Research Center, School of Chemistry and Chemical Engineering, Shanghai Jiao Tong University, Shanghai 200240, P. R. China

*k.wang@sjtu.edu.cn

Experimental details

Material synthesis

Synthesis of the sodium-doped nickel phosphate materials. Sodium-doped nickel phosphate nanorods (Na-NiPO NRs) were prepared by hydrothermal and calcination methods. Typically, nickel foam (NF) was ultrasonically cleaned with 6.0 M HCl solution for 2 h, and washed thoroughly with deionized water and ethanol, respectively, followed by drying at 60 ^{o}C. Then, the treated NF was immersed in 5.0 mM $NaH_2PO_4 \cdot 2H_2O$ solution (water/ethanol = 1:1, v/v) and transferred into a 200 mL Teflon-lined stainless-steel autoclave for hydrothermal treatment at 160 ^{o}C for 80 min. After cooling to room temperature, the precursor was obtained after washing with deionized water and ethanol, respectively, followed by drying at 60 °C. After calcined at 200 ^{o}C for 4 h under the N_2 atmosphere, Na-NiPO NRs were finally obtained. As comparison, sodium-doped nickel phosphate nanoparticles (Na-NiPO NPs) were also prepared with the same process. The precursor for Na-NiPO NPs was prepared hydrothermally in an autoclave for 30 min.

Materials characterizations

Fourier transform infrared (FTIR) spectra were recorded on a PerkinElmer Paragon 1000 spectrometer. Structures and morphologies of as-prepared samples were studied by the field-emission scanning electron microscope (FESEM, NOVA Nano SEM 230, FEI, USA) and the transmission electron microscope (JEM-2100F TEM, JEOL, Japan). X-ray photoelectron spectroscopy (XPS) analyses were performed on an X-ray photoelectron spectroscope (AXIS Ultra DLD).

Electrochemical Test

All of the 2025-type Li-O_2 cells were assembled in an Ar-filled glovebox (H_2O and O_2 < 0.5 ppm) using a lithium foil anode, a glass fiber separator, a Na-NiPO@NF cathode and an electrolyte containing 1.0 M lithium bis(trifluoromethanesulfonyl) imide in tetraethylene glycol dimethyl ether (LiTFSI/TEGDME). Galvanostatic charge/discharge tests were performed in a pure O_2 atmosphere at room temperature using a battery tester (LAND CT2001). Cyclic voltammetry (CV) curves were obtained at a scan rate of 0.5 mV s^{-1} within a voltage range of 2.2 V and 4.4 V on an electrochemical workstation (CHI 660E). Electrochemical impedance spectroscopy (EIS) measurements were conducted on the same electrochemical workstation within a frequency range from 0.01 Hz to 100 kHz.

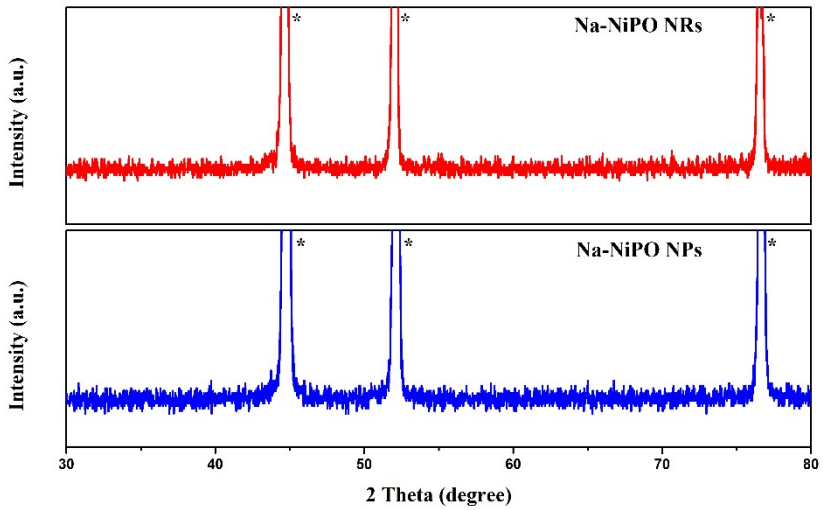

Fig. S1 XRD patterns of Na-NiPO NRs and Na-NiPO NPs.

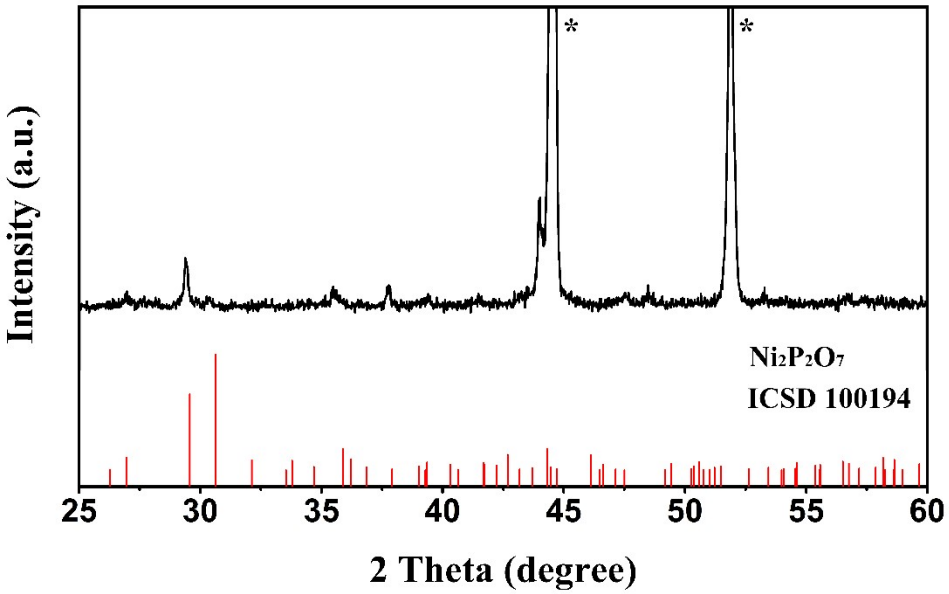

Fig. S2 XRD pattern of the synthesized material using the hydrothermal method followed by annealing at 500 ^{o}C for 2 h.

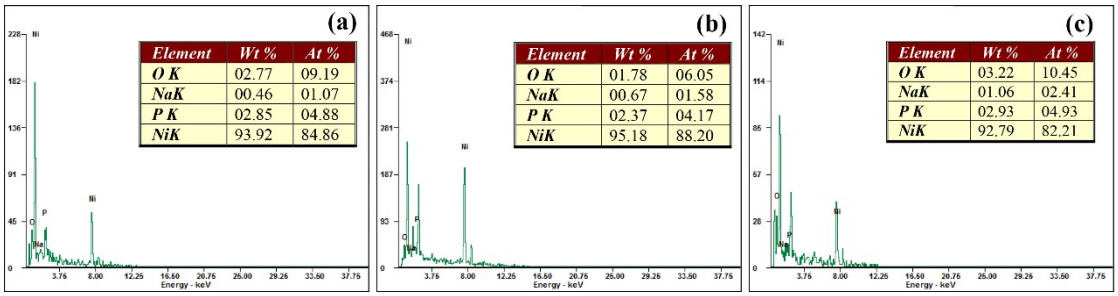

Fig. S3 Energy-dispersive X-ray analyses of precursors prepared hydrothermally on Ni foams for (a) 30, (b) 60 and (c) 80 min, respectively.

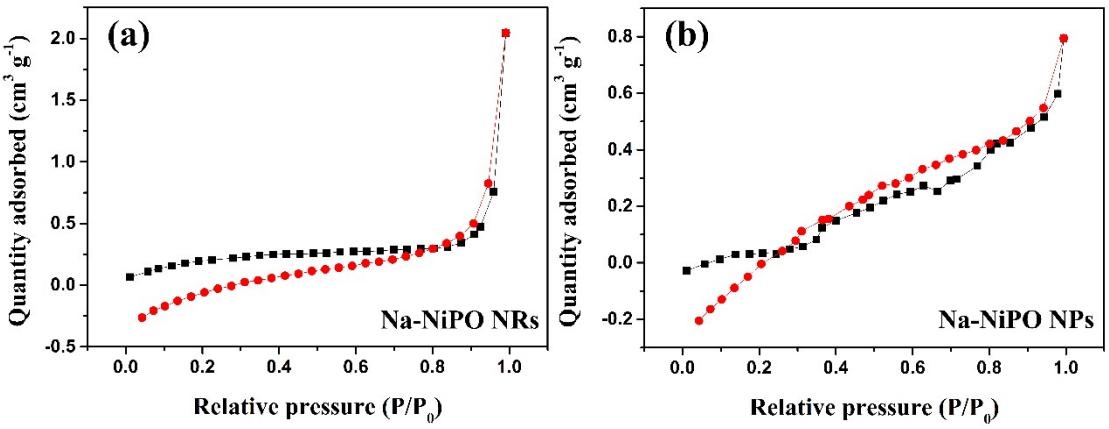

Fig. S4 Nitrogen adsorption–desorption isotherms of (a) Na-NiPO NRs and (b) Na-NiPO NPs respectively.

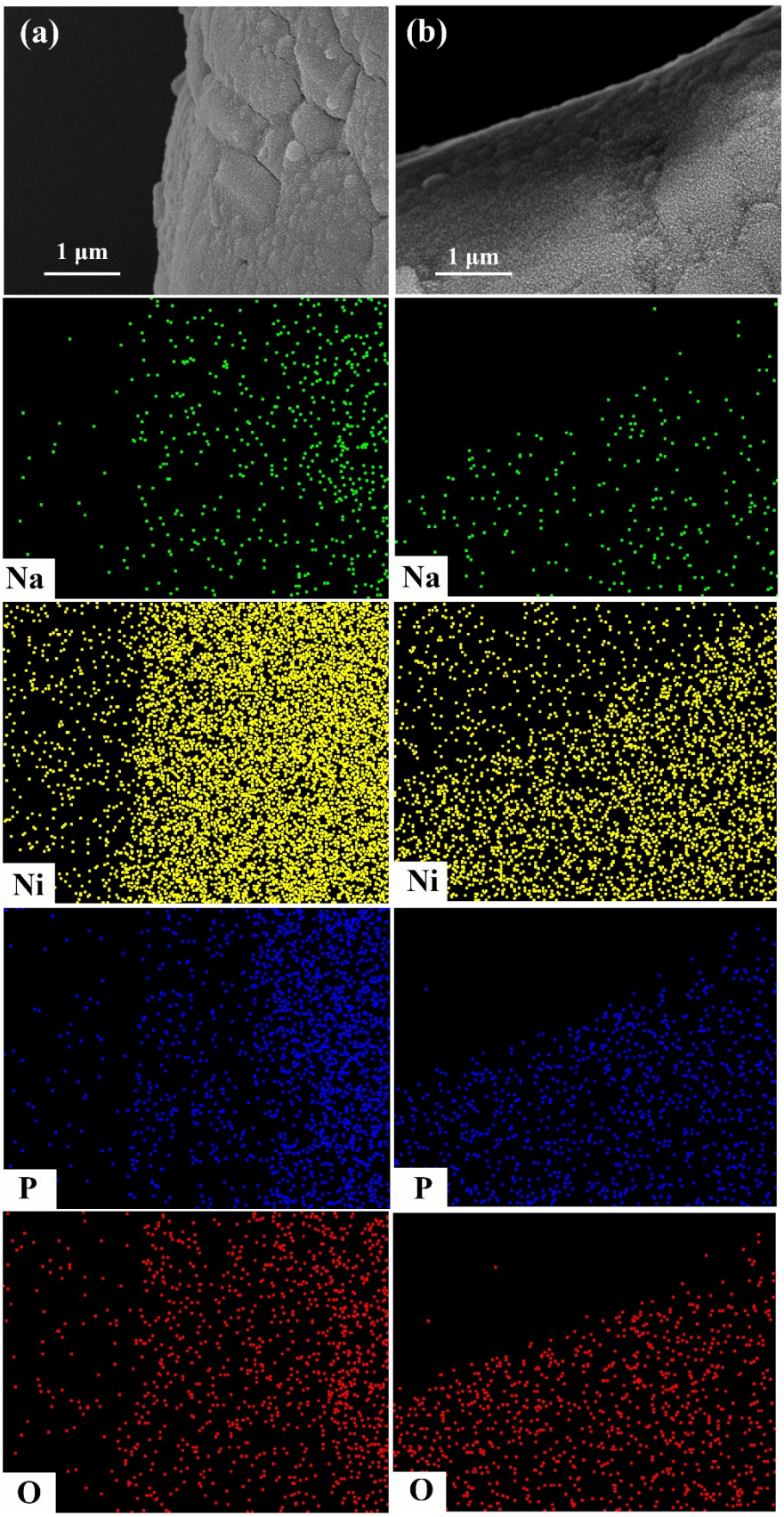

Fig. S5 Elemental mapping of (a) Na-NiPO NPs and (b) Na-NiPO NRs.

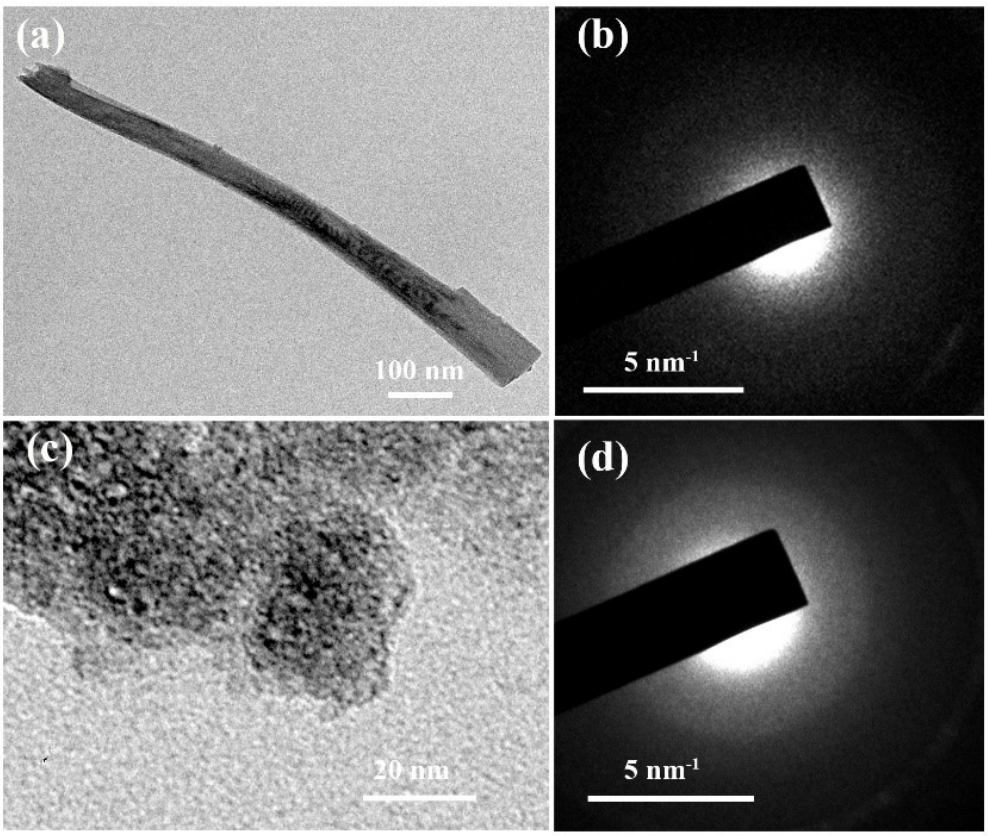

Fig. S6 (a) TEM image and (b) SAED pattern of Na-NiPO NRs. (c) TEM image and (d) SAED pattern of Na-NiPO NPs.

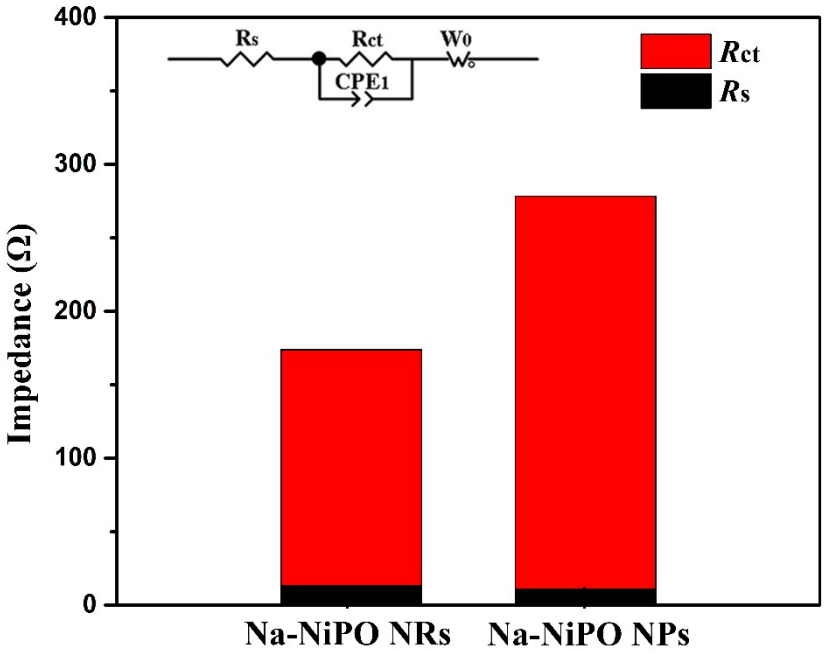

Fig. S7 Fitting results for Nyquist plots of Li-O_2 batteries with Na-NiPO NRs and Na-NiPO NPs.

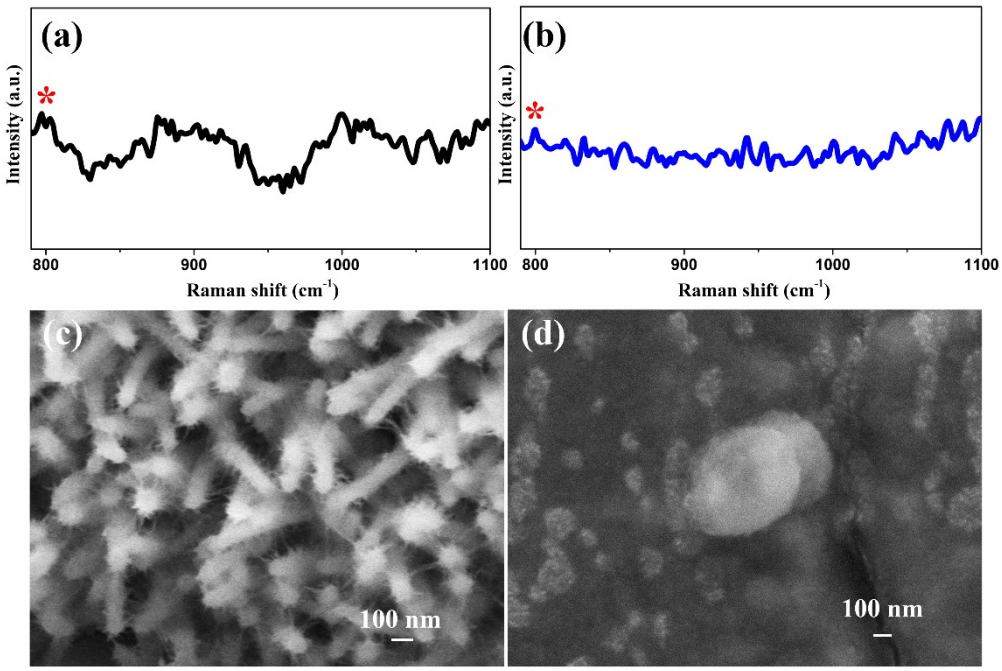

Fig. S8 Raman spectra of discharged (a) Na-NiPO NRs and (b) Na-NiPO NPs at 100 mA g^{-1}. SEM images of the discharged (c) Na-NiPO NRs and (d) Na-NiPO NPs at 100 mA g^{-1}.

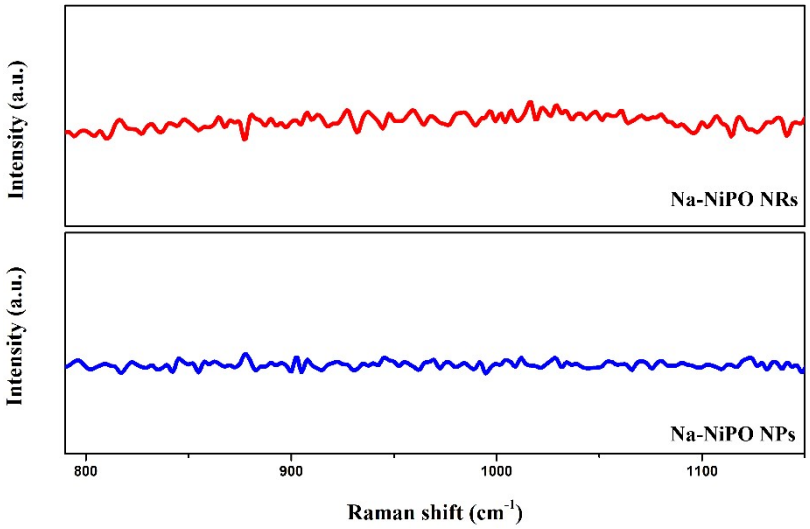

Fig. S9 Raman spectra of the Na-NiPO NRs and Na-NiPO NPs charged to 500 mAh g^{-1}.

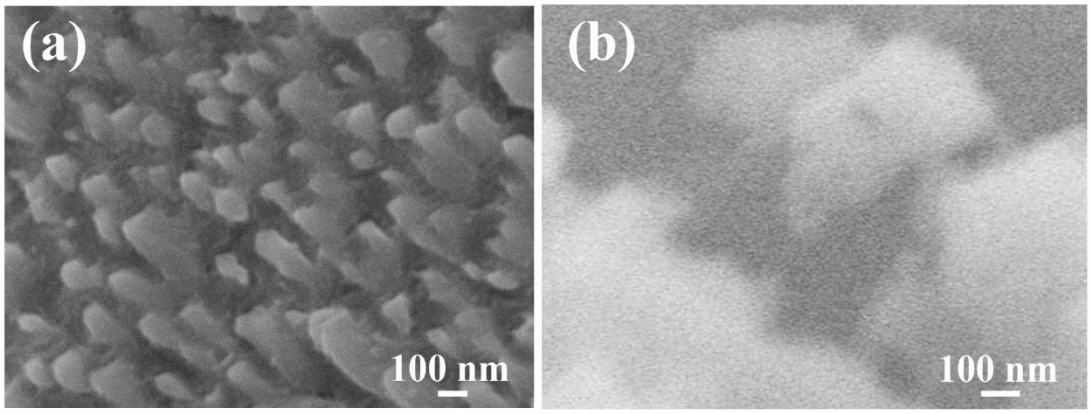

Fig. S10 SEM images of recharged (a) Na-NiPO NRs and (b) Na-NiPO NPs after the 50th cycle**.**